Pax3 induces neural circuit repair through a developmental program of directed axon outgrowth.

Jara JS[1], Avci HX[1], Kouremenou I[1], Doulazmi M[1], Bakouche J[1], Dubacq C[2], Goyenvalle C[1], Mariani J[1], Lohof AM[1], Sherrard RM[1]

1: Sorbonne Université & CNRS, IBPS-B2A, UMR 8256 Biological Adaptation and Ageing

2: Sorbonne Université, IBPS-NPS, CNRS UMR 8246 and INSERM U1130, Neurosciences Paris Seine

Running title: Pax3 induces axon outgrowth

Corresponding author:

Rachel M Sherrard

UMR 8256 B2A Biological Adaptation and Ageing

Boite 256, Sorbonne Université

9 Quai St Bernard, 75005, Paris

email: rachel.sherrard@sorbonne-universite.fr

ABSTRACT

Although neurotrophins can reorganise surviving neuronal connections after a lesion, clinical improvement is minimal and underlying mechanisms ill-defined, which impedes the development of effective treatment strategies. Here we show that the neurotrophin brain derived neurotrophic factor (BDNF) upregulates the transcription factor Pax3, which in turn induces axon outgrowth and synaptogenesis to repair a neural circuit. This repair depends on Pax3 increasing polysialic acid-neural cell adhesion molecule (PSA-NCAM), which is both essential for, and mediates the amount of, reinnervation. Pax3 acts pre-synaptically: its expression in reinnervating neurons induces significant axonal growth, and Pax3 knockdown abolishes reinnervation induced by BDNF, either endogenous BDNF expression during spontaneous developmental repair, or exogenous BDNF treatment in the mature nervous system. This is a novel role for Pax3. We propose that neuronal Pax3 induces PSA-NCAM expression on axon terminals to increase their motility and outgrowth, thereby promoting neural circuit reorganisation and repair.

Keywords Reinnervation; collateral sprouting; Pax3; PSA-NCAM; sialtransferase; olivocerebellar path; climbing fibre;

INTRODUCTION

Repairing neuronal circuit damage or dysfunction remains a major challenge in biomedical science, because the poor growth properties of adult neurons and inhibitory extracellular molecules prevent effective axon outgrowth (Lewis et al., 2013; Rodemer et al., 2020). Moreover, neurons are lost during trauma or neurodegenerative disease, so re-growing the identical circuit is not possible, and functional recovery requires the structural reorganisation of remaining undamaged axons (Asboth et al., 2018; Bennett et al., 2018). Such post-lesion circuit reorganisation is a phenomenon of the developing brain (Spear, 1995; Tillakaratne et al., 2010; Willson et al., 2008). Unfortunately, treatment strategies to recreate developmental processes, by increasing a neuron's growth capacity (He and Jin, 2016; Ribas and Costa, 2017), or the growth-permissiveness of the cellular environment (Freund et al., 2009; Zhang et al., 2007), generally produce inaccurate connections that do not restore circuit function and may even have deleterious effects (Khan and Smith, 2015). It is therefore imperative to identify molecules that can promote axon growth while also allowing appropriate cellular targeting and synapse formation, as would occur during development.

The neurotrophin family of growth factors has fundamental roles in neural development and consequently has been widely studied in neural circuit repair. While neurotrophins may improve neuronal survival and axon sprouting, there is little clinical benefit (Kelamangalath and Smith, 2013; Meeker and Williams, 2015). It is only when neurotrophins, in particular BDNF (brain-derived neurotrophic factor), are examined in their developmental roles — either inducing neurons to extend axons (Fornaro et al., 2020; Vavrek et al., 2006) or attracting axons as a target derived factor (Dixon and Sherrard, 2006; Sherrard and Bower, 2001) — that axon collateral growth reorganises spared connections effectively to improve function. The effect of BDNF is highly dose-dependent; prolonged high dosage induces pathological pain and spasticity (Fouad et al., 2013; Khan and Smith, 2015) but more physiological concentrations reduce these adverse effects (Khan and Smith, 2015; Lee-Hotta et al., 2019), probably because of differential signalling cascades through BDNF receptors. To promote beneficial postlesion plasticity and avoid unwanted effects, it is necessary to identify those repair mechanisms downstream of BDNF which allow focussed action without excessive sprouting, and thus fewer inaccurate neural connections.

In this study we examined molecular pathways downstream from BDNF using an experimental model in which the biological effect can be readily quantified, and in which we can separate treatments to act *either* on axonal outgrowth (presynaptic) *or* by target attraction (postsynaptic). This is postlesion repair of the olivocerebellar path (Dufor et al., 2019; Willson et al., 2008). Starting with BDNF-signalling molecules associated with olivocerebellar development, we show that cerebellar (target) BDNF increases the growth-permissive molecule PSA-NCAM throughout the olivocerebellar system. This upregulation of PSA-NCAM synthesis, in either the target cerebellum or the reinnervating inferior olive, is necessary and sufficient for reinnervation. The transcription factor Pax3, which links BDNF and PSA-NCAM (Kioussi and Gruss, 1994; Mayanil et al., 2000; Schüller et al., 2006), is also upregulated during reinnervation, but only in the (afferent) inferior olive. Olivary expression of Pax3 is required for reinnervation to take place, and its upregulation can induce olivary axon (climbing fibre) outgrowth.

Although Pax3 is strongly expressed in the early-developing hindbrain, where it regulates neuronal differentiation and regionalisation (Vennemann et al., 2008), this is the first demonstration that it is involved in axonal outgrowth in the mammalian brain. Finally, to determine whether these mechanisms were relevant to developmental plasticity, we show that decreasing either cerebellar PSA-NCAM or olivary Pax3 during development sharply reduces the spontaneous postlesion repair which is characteristic of the immature system. These data demonstrate that molecules downstream of BDNF, acting on a subset of mechanisms (e.g. axonal outgrowth *or* target attraction), may provide a more-focussed and therefore more effective approach to produce circuit repair. This knowledge may facilitate the development of new treatment strategies for human neurological disease.

RESULTS

We used denervated co-cultured hindbrain explants (Figure S1) to elucidate downstream mechanisms of BDNF that underlie appropriately-targeted neural circuit repair. In this model, target-derived BDNF induces intact host climbing fibres to grow collaterals into a graft hemicerebellum and reinnervate Purkinje cells (Dufor et al., 2019; Letellier et al., 2009).

BDNF injection into the graft hemicerebellum increases terminal sprouting from intact (host) climbing fibres

First we confirmed that olivocerebellar reinnervation *ex vivo* follows the same maturational changes as *in vivo*: spontaneous reinnervation during development (lesion at 9 DIV, ~P3) and BDNF-induced reinnervation in the maturing system (lesion at 21 DIV, ~P15; Sherrard et al., 1986; Willson et al., 2008). Cultured cerebellar plates (graft) were removed from their brainstem (denervation) and apposed to the cerebellar plates of an intact explant (host) for reinnervation (Fig S1A; Dufor et al., 2019; Letellier et al., 2009) and those lesioned at 21 DIV were treated with BDNF or vehicle. After 10 days co-culture, we observed VGLUT2-labelled terminals around Purkinje cell somata and dendrites (Fig S1B) in hemicerebella lesioned at 9DIV and 21DIV treated with BDNF, consistent with functional climbing fibre reinnervation (Letellier et al., 2009). There was no such labelling in vehicle-treated 21DIV lesion hemicerebella. Reinnervation density was greater after lesion at 9 DIV than at 21 DIV, and at both ages reinnervation decreased with increasing laterality into the hemicerebellum (Fig S1C), as demonstrated *in vivo* (Dixon and Sherrard, 2006; Willson et al., 2008). This suggests that cerebellar factors, of which BDNF is one, act on the olivary climbing fibre afferents to induce their outgrowth.

We therefore studied the initial effects of BDNF on host climbing fibre terminals that might explain their subsequent growth and reinnervation of graft Purkinje cells. We injected the inferior olive with lentivirus expressing GFP (LV-GFP) to visualize climbing fibre arbors in the host hemicerebellum (Fig 1A) and compared their structure in intact explants (control) and explants co-cultured at 21 DIV treated with exogenous BDNF (or vehicle). Host climbing fibre arbors were modified 24h after co-culture. Compared to vehicle-treated or control (no apposed graft) explants (Fig 1B), BDNF-treated arbors had many thin long horizontal branches. In particular, BDNF treatment resulted in more climbing fibres with horizontal branches greater than 40 μm long (Fig 1B&C).

To test whether this sprouting was due to diffusion of BDNF into the host hemicerebellum to affect these intact climbing fibre terminals, we used c-fos immunolabelling 1½h after treatment to identify BDNF-stimulated cells. C-fos labelling was only detectable in the BDNF-treated *graft* cerebellar hemisphere (Fig S2), and not in the adjacent host hemicerebellum,

nor in vehicle treated grafts, suggesting that the action of BDNF was local within the denervated tissue.

BDNF-induced olivocerebellar reinnervation requires PSA-NCAM

To identify *how* BDNF induced sufficient climbing fibre outgrowth to reach and reinnervate Purkinje cells in the grafted hemicerebellum, we examined molecules associated with neural circuit development. Polysialic acid (PSA)-NCAM is highly expressed in early development, promoting axonal growth (Rutishauser, 2008). It is also involved in climbing fibre maturation and post-lesion cerebellar plasticity (Avella et al., 2006; Zhang et al., 2007).

We measured PSA-NCAM during reinnervation in the cerebellar plate and inferior olive (Table 1). In control tissue, PSA-NCAM concentration decreased during maturation, being approximately halved in the cerebellar plate and inferior olive between 21-26DIV (~P15-20, Table 1a&b). In lesioned/cocultured explants PSA-NCAM levels were maintained by BDNF application so that by 4 days post-lesion PSA-NCAM was x1.5-2 greater than control tissue (Table 1b: 26DIV C vs BDNF). Moreover, in a lesioned/isolated cerebellar plate PSA-NCAM expression did not increase after BDNF treatment (Table 1a). Thus, increased PSA-NCAM parallels the greater climbing fibre sprouting in BDNF-treated explants.

To determine whether increased PSA-NCAM is actually involved in olivocerebellar reinnervation, we altered PSA-NCAM levels in the target (cerebellum) or reinnervating (inferior olive) regions and re-evaluated climbing fibre reinnervation. First, we treated graft hemicerebella with the sialidase EndoN, to remove PSA from NCAM. EndoN reduced PSA-NCAM in lesioned-BDNF-treated hemicerebella (Table 1a) and halved BDNF-dependant reinnervation (Fig 2A). In contrast, overexpression of cerebellar *Sia2*, a sialtransferase that adds PSA to NCAM (Rutishauser, 2008), induced the same percentage of Purkinje cell reinnervation as did BDNF injection (Fig 2A). However, *Sia2* was not overexpressed in the target Purkinje cells themselves (Fig S3), which suggests that PSA-NCAM acts by providing a growth permissive extracellular environment. Next, we overexpressed *sia2* in the reinnervating inferior olive 24 hours after co-culture (Fig 2B). Olivary *Sia2* overexpression increased climbing fibre-Purkinje cell reinnervation by 50% compared to cerebellar BDNF, but these two treatments did not have additive effects (Fig 2B). In contrast, olivary overexpression

of another sialtransferase isoform, *sia4* which is preferentially expressed in the mature nervous system (Rutishauser, 2008), was less effective (Fig S4). Also, modifying *Sia2* or *Sia4* with a 3'UTR variation, to target the mRNA to axon terminals, did not further improve reinnervation (Fig S4).

Taken together these data indicate that BDNF induces climbing fibre reinnervation by increasing PSA-NCAM in the olivocerebellar environment. Increased PSA on the reinnervating axon is even more effective in promoting climbing fibre axon outgrowth and synaptogenesis.

Paired homeobox transcription factor Pax3 induces olivocerebellar reinnervation

We next looked for the link between BDNF and increased PSA-NCAM. In cerebellar neuronal culture BDNF upregulates *Pax3* (Kioussi and Gruss, 1994), a transcription factor expressed in the immature cerebellum and brainstem (Schüller et al., 2006; Vennemann et al., 2008), and which upregulates *Sia2* and *Sia4* (Mayanil et al., 2000). *In silico* searches confirmed the link between BDNF and Pax3 expression, showing connections both through BDNF-TrkB signalling (Kamaraju et al., 2002; Yin et al., 2015) and direct protein-protein interactions (Chang et al., 2008; Grados et al., 2014; Fig S5A).

We therefore measured *Pax3* expression in the cerebellar graft and inferior olive 1 - 48 hours after co-culture and cerebellar BDNF treatment. Inferior olivary *Pax3* mRNA expression transiently increased 24h post BDNF and was followed by increased Pax3 protein at 48h (Fig 3A, B). There were no changes in Pax3 mRNA or protein in the cerebellum, nor in vehicle-treated controls. These results indicate that increased olivary Pax3 occurs in response to the cerebellar BDNF treatment, at a time when olivary neurons are actively extending axonal branches toward the graft.

To test for a role of Pax3 upregulation in olivocerebellar reinnervation, we altered olivary *Pax3* and observed dramatic changes in climbing fibre reinnervation. *Pax3* knockdown effectively abolished BDNF-induced reinnervation (Fig 3C). Conversely, olivary *Pax3* overexpression induced Purkinje cell reinnervation (Fig 3C) with functional climbing fibre synapses (Fig S6). The amount of reinnervation was similar to that induced by BDNF, but *Pax3* was also additive to the effect of BDNF (Fig 3C). Finally, we verified that Pax3-induced effects on climbing fibres

resembled those induced by BDNF: 24 hours after olivary *Pax3* overexpression there was extensive sprouting of host climbing fibre horizontal branches (Figure 4A), and cerebellar PSA-NCAM was increased (Fig 4B). The importance of PSA-NCAM in olivocerebellar reinnervation is indicated by the presence of PSA-NCAM on reinnervating axonal growth cones (Figure 4C).

To verify that Pax3 is a necessary component of BDNF-induced neural circuit repair, we examined its role in repair during development, which occurs spontaneously in the olivocerebellar path (Sherrard et al., 1986; Sugihara et al., 2003; Willson et al., 2008; Zagrebelsky et al., 1997) through action of endogenous BDNF (Sherrard et al., 2009). After lesion and co-culture in immature explants equivalent to post-natal day 3 (P3, 9 DIV) to induce spontaneous climbing fibre-Purkinje cell reinnervation (Fig S1), *Pax3* was rapidly upregulated in the inferior olive by 6h (Fig 5A). After ten days, there was robust spontaneous climbing fibre-Purkinje cell reinnervation to over 50% of Purkinje cells in the grafted cerebellar plate (Fig 5B); this result is similar to that seen for postlesion repair *in vivo* (Sherrard et al., 1986; Willson et al., 2008; Zagrebelsky et al., 1997). Moreover, this reinnervation was significantly reduced by either EndoN treatment of the grafted cerebellar plate to reduce PSA-NCAM, or *Pax3* knockdown in the host olivary neurons (Fig 5B). Finally, *in silico* searching showed that Pax3 target genes are highly over-represented in the Gene Ontology functions axon extension (GO:0048675), axon regeneration (GO:0031103) and synapse (GO:0051963; Fig S5B) supporting its role in BDNF-induced neural circuit repair.

These data show for the first time that Pax3 can induce axonal growth and synaptogenesis in the mammalian nervous system and is a necessary component downstream of BDNF.

DISCUSSION:

In this study we used our *ex vivo* model of the olivocerebellar path to understand how BDNF promotes post-lesion reorganisation of remaining intact neural circuits to reinnervate denervated targets. We show that BDNF-induced axon collateral growth can be reproduced by presynaptic neuronal expression of the transcription factor Pax3. Pax3 rapidly induces olivary axonal sprouting and subsequent collateral elongation in parallel with increased PSA-

NCAM. We also show that both Pax3 and PSA-NCAM are *necessary* for BDNF-induced reinnervation to take place.

Pax3 induces olivocerebellar axonal outgrowth to reinnervate Purkinje cells

A key discovery of this study is the capacity for Pax3 to induce axonal outgrowth and neural circuit repair. Increased expression of *Pax3* in the inferior olive induced post-lesion Purkinje cell reinnervation by functional climbing fibres, to the same level as that induced by BDNF. Accordingly, *Pax3* knockdown effectively abolished the climbing fibre-Purkinje cell reinnervation normally induced by BDNF application. This is the first demonstration that Pax3 can induce axonal growth and neosynaptogenesis in both developing and mature mammalian central nervous system.

Pax3 is a paired-box transcription factor that is critically involved in the early development of the central nervous system and neural crest, regulating the proliferation of neural precursors in the neural tube and Schwann cell precursors in peripheral nerves (Boudjadi et al., 2018). There are no prior reports of links between Pax3 and axonal outgrowth, only its re-expression in damaged Schwann cells after sciatic nerve lesion (Vogelaar et al., 2004) and associated myelination (Kioussi et al., 1995). However, *in silico* searches and text-mining revealed that a large number of genes with Gene Ontology functions of axon extension, regeneration, and synaptogenesis, contain Pax3 binding sequences in their promoter regions; and many of these are expressed in the olivocerebellar system (Figure S5B). Our data also provide a potential mechanism of action, since Pax3 increased PSA-NCAM in the grafted cerebellar plate, providing a growth-permissive environment; this result is consistent with Pax3's upregulation of the sialtransferases *sia2* and *sia4* (Mayanil et al., 2000).

Our data also suggest that Pax3 is an integral part of the BDNF repair program. Not only does BDNF upregulate *Pax3* expression in neuronal culture (Kioussi and Gruss, 1994), but we observe Pax3 upregulation in the inferior olive both by BDNF treatment after lesion/coculture at 21DIV *and* during reinnervation after lesion/coculture at 9DIV, which occurs spontaneously through the action of endogenous BDNF (Sherrard et al., 2009). The effect of Pax3 can be further potentiated by cerebellar BDNF (Figure 3C), which supports the hypothesis that Pax3-promoted axonal outgrowth is one mechanism by which BDNF induces olivocerebellar

reinnervation; but that other signalling cascades activated by BDNF-TrkB (Liu and Snider, 2001) are also involved. Furthermore, the initial climbing fibre sprouting and subsequent arbors are morphologically similar to transcommissural olivocerebellar reinnervation induced after this lesion *in vivo* (Dixon and Sherrard, 2006; Sugihara et al., 2003; Willson et al., 2008; Zagrebelsky et al., 1997). Climbing fibre terminals can sprout and grow through the unmyelinated cerebellar molecular layer to reinnervate adjacent denervated Purkinje cells (Dhar et al., 2016; Rossi et al., 1991); as indeed we observed in this study in vehicle-treated graft cerebella (Fig 1A). However, BDNF is required for long distance olivocerebellar axon collateral extension and climbing fibre-Purkinje cell reinnervation, either endogenous BDNF during development (Sherrard et al., 2009) or exogenous BDNF in the mature system (Dixon and Sherrard, 2006; Sherrard and Bower, 2001; Willson et al., 2008). Here we demonstrate that Pax3 is an essential component of this process. We also show that the source of these collaterals are the horizontal branches of climbing fibre arbors (Fig 1). Thin horizontal climbing fibre terminal branches have been previously described (Nishiyama et al., 2007; Sugihara et al., 1999), although their function is unknown as they do not form synaptic terminals (Nishiyama et al., 2007). Their importance is illustrated by their presence on the newly-formed reinnervating arbors (Dhar et al., 2016; Sugihara et al., 2003). The extensive branching of these horizontal branches induced by either BDNF application or Pax3 expression (Figs 1C and 4B) is entirely consistent with the 15-fold increase in terminal arbors supported by reinnervating transcommissural olivocerebellar collaterals observed *in vivo* in the immature system (up to 89 collaterals per climbing fibre; (Sugihara et al., 2003).

Pax3 induced olivocerebellar reinnervation is a developmental plasticity program

The results of this study also suggest that Pax3 is part of a developmental repair program, of which collateral outgrowth from remaining intact axons is a major component (Spear, 1995; Tillakaratne et al., 2010; Willson et al., 2008). Pax3 is involved in very early neural precursor development (Boudjadi et al., 2018). It is strongly expressed in the embryonic hindbrain from E8.5, where it regulates regional developmental genes (Vennemann et al., 2008) ; however Pax3 expression ceases by E12-13 (Goulding et al., 1991), a time when cerebellar macroneurons are differentiating, but migration and axonal growth have barely begun (Leto et al., 2016). Thus, Pax3 is unlikely to have a critical role in axonal outgrowth during normal olivocerebellar development.

In contrast, our data support a role for Pax3 in a developmental plasticity program. First, spontaneous reinnervation after lesion and coculture at 9DIV (~P3) is blocked by knock-down of inferior olivary *Pax3* (Fig 5B). Also, inferior olivary *Pax3* overexpression in the maturing system induces rapid sprouting of climbing fibre horizontal branches within 24h (Fig 4B), similar to the action of BDNF. This is consistent with rapid spontaneous sprouting seen in the molecular layer 18h after pedunculotomy *in vivo* early in development (Zagrebelsky et al., 1997) and reinnervation of denervated Purkinje cells within 24-48h (Lohof et al., 2005). This rapid climbing fibre sprouting is followed by increased cerebellar PSA-NCAM (Fig 4A), thus mimicking the PSA-NCAM-rich environment during olivocerebellar maturation (Avella et al., 2006).

Increased PSA-NCAM is a final common pathway for climbing fibre-Purkinje cell reinnervation

The second component of BDNF-induced postlesion repair revealed in our model, consistent with reactivating elements of developmental plasticity, is the involvement of PSA-NCAM. PSA-NCAM is a canonical component of neurodevelopment and its plasticity, and in our model we confirm that 1) young lesioned explants have high levels of PSA-NCAM (Table 1A) associated with high spontaneous Purkinje cell reinnervation (Fig 5B); 2) BDNF application to more mature lesioned-cocultured explants increases PSA-NCAM in the inferior olive from 2 days (Table 1b), when reinnervating climbing fibre collaterals are growing into the denervated hemicerebellum; and 3) increased PSA-NCAM synthesis, particularly in the reinnervating inferior olive, induces extensive climbing fibre-Purkinje cell reinnervation (Fig 2). This reinnervation is reduced if PSA-NCAM is removed (by EndoN), and BDNF does not increase PSA-NCAM in the absence of reinnervation, i.e. in an isolated hemicerebellar anlage (Table 1a).

This importance of PSA-NCAM on the reinnervating olivocerebellar axons, compared to within the cerebellum, is illustrated by greater BDNF-induced upregulation of PSA-NCAM in the inferior olive (Table 1b), and greater climbing fibre-Purkinje cell reinnervation when PSA-NCAM is increased in the inferior olive (cf Fig 2A vs B). Although PSA-NCAM is generally considered a permissive environment that allows axon outgrowth (Zhang et al., 2007), there

is increasing evidence that its presence on the *growth cone* is essential for directing axon extension, both during development (Schiff et al., 2011) and reinnervation (Bonfanti, 2006). Given that *in vivo* climbing fibre-Purkinje cell reinnervation displays appropriate topographic organization (Sherrard & Bower, 1997; Zagrebelsky et al 1997; Sugihara et al 2003), we suggest that increasing Pax3 expression, to increase PSA-NCAM on reinnervating axon terminals, may better provide effective (i.e. appropriately targeted) neural circuit repair without the adverse effects induced by BDNF administration or by generalized increases in PSA-NCAM throughout the neural pathway.

In conclusion, BDNF induces axon outgrowth and targeted neosynaptogenesis in olivocerebellar reinnervation, both in vivo and ex vivo (Dixon and Sherrard, 2006; Dufor et al., 2019; Sherrard and Bower, 2001; Willson et al., 2008). We show here that this reinnervation depends on the transcription factor Pax3 and its downstream target, PSA-NCAM. Our data suggest that BDNF induces Pax3 expression which triggers PSA-NCAM synthesis; when present on axon terminals, PSA-NCAM promotes target-directed axon growth that contributes to neural circuit repair. This is a novel role for Pax3, but its ability to activate phenomena of directed axon outgrowth, in both developmental and regenerative situations, opens the possibility of its application to a range of biological questions and clinical challenges.

Author contributions: The project was designed by RMS and JSJ; explant experiments were performed by JSJ, HXA, IK, AML and RMS; biochemistry and viral vector construction were done by HXA and JB; qPCR was undertaken by CD and HXA; ELISA was done by CG; in silico searches were made by MD; data analysis and interpretation were performed by JSJ, HXA, IK, AML, and RMS. All authors contributed to the final article.

The authors declare no competing interests.

Acknowledgements

This project was funded by the Institut pour la Recherche sur la Moelle épinière et l'Encéphale, and the Fondation pour la Recherche Médicale. We would like to thank Pr Allan Tobin for all his valuable advice on the manuscript, and Mme Corinne Nantet for help cutting histology sections.

METHODS

RESOURCE AVAILABILITY

Lead Contact

Further information and requests for resources and reagents should be directed to and will be fulfilled by the Lead Contact, Rachel M Sherrard (rachel.sherrard@sorbonne-universite.fr)

Materials Availability

This study did not generate new unique reagents.

Data and Code Availability

This study did not generate new code.

EXPERIMENTAL MODEL AND SUBJECT DETAILS

Animals

Timed-pregnant RjOrl:Swiss mice were purchased from Janvier (France) and housed under standard laboratory conditions with 12 hours light/dark cycle and free access to food and water. Age and number of mouse embryos used for each experiment are detailed in the figure legends. Sex of embryos used was not tested. All housing and procedures were approved by the Comité National d'Ethique pour les Sciences de la Vie et de la Santé (N° 1492-02) and performed in accordance with the guidelines established by the European Communities Council Directive (2010/63/EU).

METHOD DETAILS

Organotypic cultures

Mouse hindbrain explant cultures were performed at E14, as described previously (Dufor et al., 2019; Letellier et al., 2009). Briefly, pregnant mice were anaesthetised with isoflurane and euthanised by cervical dislocation. Embryos were removed from the uterus and their heads placed into ice-cold Gey's balanced salt solution (Eurobio, France) with 5 mg/ml glucose, and brains were quickly dissected out. The hindbrain (including the cerebellar anlage and the inferior olive nucleus), was isolated and the meninges removed. Explants were transferred

onto 30 mm Millipore culture membranes (pore size 0.4 µm; Millicell CM, Millipore, MA) and placed in six-well plates with 1ml/well of medium containing 50% basal medium with Earle's salts, 25% Hank's Balance Salt Solution, 25% horse serum (all Invitrogen, CA), 1 mM L-glutamine, and 5 mg/ml glucose. Explants were cultured at 35°C in a humidified atmosphere with 5% CO2. The day of dissection was 0 days *in vitro* (0 DIV). The medium was replaced every 2–3 days. In each litter, explants were semi-randomly assigned to different experimental groups, so that each litter contributed to several groups and each group contained explants from different litters.

Cerebellar denervation and explant injection

To denervate cerebellar tissue and induce olivo-cerebellar reinnervation, the cerebellar plates were removed from their brainstem at 9 or 21 DIV (equivalent to P3, when olivocerebellar reinnervation is spontaneous, or P15, when reinnervation requires BDNF; Willson et al., 2008) and apposed (graft) to intact (host) cerebellar tissue for co-culture. In this configuration, reinnervating olivary axons must grow through white matter and pass neurons of the deep cerebellar nuclei, which is similar to in vivo post-pedunculotomy repair (Sugihara et al., 2003).

21 DIV co-culture: Twenty-four hours after co-culture at 21 DIV, some cerebellar plates were treated with 1µl (4µM) recombinant human brain derived neurotrophic factor (hBDNF; Alomone, 0.1% BSA in H_2O). To investigate mechanisms associated with climbing fibre-Purkinje cell reinnervation, co-culture explants also received other treatments: (1) 350 IU of neuraminidase EndoN (AbCys, France) injected onto the graft (denervated) hemicerebellum on +1 (22 DIV) and +7 (28 DIV) days to digest PSA from PSA-NCAM; (2) lentiviral mediated gene transfer to induce over-expression of Sia2, Sia4, Pax3, or GFP in either the graft cerebellar plate (1µl) or inferior olive (4x50nl), injected +1 day after co-culture (22 DIV; see Supplementary methods for virus production); (3) inferior olivary injection (4x50nl) of lentivirus containing pooled siPax3/hPax3/Pax3i/GFP (LVsiPax3; Gentaur, France) to knock-down Pax3 expression, injected +1 day after co-culture (22 DIV).

9 DIV co-culture: Grafted hemicerebella of some explants were treated, as above, with: (1) cerebellar Endo-N at +1 (10 DIV) and +7 (16 DIV) days; or (2) inferior olivary injection of LVsiPax3 at +1 day (10DIV).

Immunohistochemistry

We used double or triple fluorescent immunolabelling to identify the presence or absence of climbing fibre reinnervation, virally-transfected neurons, and different cell populations in the cerebellum or inferior olivary nucleus (primary antibodies are identified in Table S1). Explants were fixed for 4 hours with 4% PFA in 0.1 M PBS at various post-lesion survival times. Some explants were cryo-protected in 10% sucrose in 0.1 M PBS, embedded in 7.5% gelatine with 10% sucrose for transverse cryo-sectioning (10 µm thick). Explants or cryosections were incubated overnight at 4°C with different combinations of primary antibodies. Immunolabelling was visualized with FITC-, Cy5-, or Cy3-conjugated species-specific donkey secondary antibodies (1:200; Jackson ImmunoResearch Laboratories, West Grove, PA). Finally, sections or explants were mounted in Mowiol (Calbiochem, La Jolla, CA) and examined using epifluorescence microscopy (Leica DM6000); or mounted in CFM3 (Citifluor Ltd, UK) for confocal (Leica SP5, Vienna, Austria) imaging of climbing fibre transverse branches.

Histological Analysis

The amount of climbing fibre reinnervation was measured 10 days after treatment (with BDNF, EndoN, or LV injection). We quantified the number of calbindin-positive Purkinje cells (soma and primary dendrites) colocalised with VGLUT2 per field of view (grid) and expressed as percentage Purkinje cells per field. This quantification was made systematically on z-stacks taken in rows through the cerebellar graft with increasing distance from the host-graft interface. Climbing fibre quantification was made on these z-stacks, hiding each colour channel as necessary to ensure VGLUT2 puncta were not missed. Data from rows 1 and 2 were defined as a proximal zone, and those from rows 3-5 were defined as a distal zone.

Protein analysis: Western Blot and ELISA

Cerebellar plates or inferior olivary tissue were taken from explants during development from 9 - 35 DIV and at 1, 2, 4, or 12 days post-lesion. Tissue was homogenized in 500 µl of lysis buffer (pH; 120 mM NaCl; 50 mM TRIS, 1 mM EDTA; 25 mM NaF; 1 mM Na_3VO_4; 0.5% SDS), sonicated and centrifuged (14 000 rpm, 30 min) and the supernatants were analyzed by ELISA or western blot.

PSA-NCAM concentration was measured using an ELISA kit (PSA-NCAM ELISA ABC0027B, Eurobio France) according to manufacturer's instructions. Samples were run in duplicate.

Pax3 protein was measured by western blot; 30 µg of total protein was separated by SDS-PAGE, transferred onto PVDF membranes and probed with anti-Pax3 (1:250; R&D systems) and then anti-β-actin (1:1000; Abcam). Bound antibody was visualised using HRP-conjugated anti-mouse secondary antibody (Amersham Biosciences) and ECL Advance for chemiluminescence (2 minutes exposure time; Amersham Biosciences). Bands were identified by size (Pax3: 53 kDa; βactin: 42 kDa), intensities were measured (ImageJ, Gelplot macro) and normalised against the amount of β-actin in each lane.

qRT-PCR

RNA was extracted from either the cerebellar plate or the inferior olivary region of co-cultured or control explants 6 - 96h post lesion and co-culture. Tissue from 6 cerebellar plates or inferior olive regions were pooled to obtain each sample. Total RNA was extracted using Trizol (Life Technologies) according to manufacturer's instructions (Chomczynski and Sacchi, 1987)) and RNA concentration was measured by a NanoDrop 1000 Spectrophotometer (Thermo Scientific, Waltham, MA, USA) before being stored at -80°C.

200ng of total RNA was reverse transcribed in 20µl using a High Capacity cDNA Reverse Transcription Kit (Applied Biosystems). cDNA was amplified on a LightCycler® 480 (Roche Applied Bioscience, USA) in 10 µl reaction volume using SYBR Green I Master Mix (annealing temperature 58 °C, 50 cycles). Housekeeper genes were TUB5 and ARBP and genes of interest were *cfos* and *Pax3*. Primer sequences for each gene are found in Table S2.

All samples were amplified in triplicate and the mean was used to calculate gene expression in each tissue sample. Raw data were pre-processed with Lightcycler 480 software (Roche Applied Bioscience, USA). Target gene expression was normalised to the harmonic mean of 2 housekeeper genes.

QUANTIFICATION AND STATISTICAL ANALYSES

Statistical analyses were done using GraphPad Prism 9. Data were examined for normality and homogeneity of variance and, where necessary transformed. Inter-group comparisons were made using analysis of variance (One- or two-way ANOVA) and Bonferroni's post hoc tests; or Kruskall Wallis and Dunn's post hoc tests (if normality was not attained). The number

of climbing fibre branches was assessed using the χ^2 test. All values were stated as mean±SEM and $\alpha = 0.05$. Statistical information (test and p value) are given in the figure legends.

In silico searches were used to identify potential Pax3 function in reinnervation. To analyze Pax3's protein-protein interaction network, we used the STRING database (Search Tool for the Retrieval of Interacting Genes, http://www.string-db.org/). This database integrates text mining in PubMed, experimental/biochemical evidence, co-expression, and database association to provide an interactive platform in which connections, associations, and interactions between proteins can be assessed. An interaction network chart with a combined score >0.8 was saved and exported, and is found in Figure S5A. To complement this analysis, we combined our results with Gene Ontology (GO) terms (GO:0031103 Axon Regeneration; GO:0051963 synapse; GO:0048675 Axon Extension; GO:0044295 Axonal Growth Cone). The web-based service Pubmed was used to perform text mining, and a homemade perl script extracted all available literature related to the search query for co-citation of Pax3 and the genes from GO list. Finally, to explore the putative transcription factor-target relationships of Pax3, we used R (3.3.0) and the Bioconductor suite (3.3). We applied Biostrings (2.40) and GenomicFeatures (1.24) to determine potential transcription factor binding sequences in a selected list. Transcription factor binding matrices [position weight matrix (PWM)] were obtained from the R package MotifDb (1.14) and compared, using matchPWM (with position at 90%) to target sequences in the promoter site and for 2kb upstream.

REFERENCES:

Asboth, L., Friedli, L., Beauparlant, J., Martinez-Gonzalez, C., Anil, S., Rey, E., Baud, L., Pidpruzhnykova, G., Anderson, M.A., Shkorbatova, P., et al. (2018). Cortico-reticulo-spinal circuit reorganization enables functional recovery after severe spinal cord contusion. Nat. Neurosci. *21*, 576–588.

Avella, D., Pisu, M.B., Roda, E., Gravati, M., and Bernocchi, G. (2006). Reorganization of the rat cerebellar cortex during postnatal development following cisplatin treatment. Exp. Neurol. *201*, 131–143.

Bareyre, F.M., Kerschensteiner, M., Raineteau, O., Mettenleiter, T.C., Weinmann, O., and Schwab, M.E. (2004). The injured spinal cord spontaneously forms a new intraspinal circuit in adult rats. Nat. Neurosci. *7*, 269–277.

Bennett, S.H., Kirby, A.J., and Finnerty, G.T. (2018). Rewiring the connectome: Evidence and effects. Neurosci. Biobehav. Rev. *88*, 51–62.

Bonfanti, L. (2006). PSA-NCAM in mammalian structural plasticity and neurogenesis. Prog. Neurobiol. *80*, 129–164.

Bosman, L.W.J., Hartmann, J., Barski, J.J., Lepier, A., Noll-Hussong, M., Reichardt, L.F., and Konnerth, A. (2006). Requirement of TrkB for synapse elimination in developing cerebellar Purkinje cells. Brain Cell Biol *35*, 87–101.

Boudjadi, S., Chatterjee, B., Sun, W., Vemu, P., and Barr, F.G. (2018). The expression and function of PAX3 in development and disease. Gene *666*, 145–157.

Chang, C.-P., Stankunas, K., Shang, C., Kao, S.-C., Twu, K.Y., and Cleary, M.L. (2008). Pbx1 functions in distinct regulatory networks to pattern the great arteries and cardiac outflow tract. Development *135*, 3577–3586.

Dhar, M., Brenner, J.M., Sakimura, K., Kano, M., and Nishiyama, H. (2016). Spatiotemporal dynamics of lesion-induced axonal sprouting and its relation to functional architecture of the cerebellum. Nat. Commun. *7*, 12938.

Dixon, K.J., and Sherrard, R.M. (2006). Brain-derived neurotrophic factor induces post-lesion transcommissural growth of olivary axons that develop normal climbing fibers on mature Purkinje cells. Exp. Neurol. *202*, 44–56.

Dufor, T., Grehl, S., Tang, A.D., Doulazmi, M., Traoré, M., Debray, N., Dubacq, C., Deng, Z.-D., Mariani, J., Lohof, A.M., et al. (2019). Neural circuit repair by low-intensity magnetic stimulation requires cellular magnetoreceptors and specific stimulation patterns. Sci. Adv. *5*, eaav9847.

Fornaro, M., Giovannelli, A., Muratori, L., Guena, S., Novajra, G., and Perroteau, I. (2020). Role of neurotrophic factors in enhancing linear axonal growth of ganglionic sensory neurons *in vitro*. Neural. Regen. Res. *15*, 1732–1739.

Fouad, K., Bennett, D.J., Vavrek, R., and Blesch, A. (2013). Long-term viral brain-derived neurotrophic factor delivery promotes spasticity in rats with a cervical spinal cord hemisection. Front. Neurol. *4*, 187.

Freund, P., Schmidlin, E., Wannier, T., Bloch, J., Mir, A., Schwab, M.E., and Rouiller, E.M. (2009). Anti-Nogo-A antibody treatment promotes recovery of manual dexterity after unilateral cervical lesion in adult primates--re-examination and extension of behavioral data. Eur. J. Neurosci. *29*, 983–996.

Goulding, M.D., Chalepakis, G., Deutsch, U., Erselius, J.R., and Gruss, P. (1991). Pax-3, a novel murine DNA binding protein expressed during early neurogenesis. EMBO J. *10*, 1135–1147.

Grados, M., Sung, H.M., Kim, S., and Srivastava, S. (2014). Genetic Findings in Obsessive–Compulsive Disorder Connect to Brain-Derived Neurotropic Factor and Mammalian Target of Rapamycin Pathways: Implications for Drug Development. Drug Devel. Res. *75*, 372–383.

He, Z., and Jin, Y. (2016). Intrinsic Control of Axon Regeneration. Neuron *90*, 437–451.

Kamaraju, A.K., Bertolotto, C., Chebath, J., and Revel, M. (2002). Pax3 Down-regulation and Shut-off of Melanogenesis in Melanoma B16/F10.9 by Interleukin-6 Receptor Signaling. J. Biol. Chem. *277*, 15132–15141.

Kelamangalath, L., and Smith, G.M. (2013). Neurotrophin treatment to promote regeneration after traumatic CNS injury. Front. Biol. (Beijing) *8*, 486–495.

Khan, N., and Smith, M.T. (2015). Neurotrophins and Neuropathic Pain: Role in Pathobiology. Molecules *20*, 10657–10688.

Kioussi, C., and Gruss, P. (1994). Differential induction of Pax genes by NGF and BDNF in cerebellar primary cultures. J. Cell Biol. *125*, 417–425.

Kioussi, C., Gross, M.K., and Gruss, P. (1995). Pax3: a paired domain gene as a regulator in PNS myelination. Neuron *15*, 553–562.

Lagha, M., Sato, T., Regnault, B., Cumano, A., Zuniga, A., Licht, J., Relaix, F., and Buckingham, M. (2010). Transcriptome analyses based on genetic screens for Pax3 myogenic targets in the mouse embryo. BMC Genomics *11*, 696.

Lee-Hotta, S., Uchiyama, Y., and Kametaka, S. (2019). Role of the BDNF-TrkB pathway in KCC2 regulation and rehabilitation following neuronal injury: A mini review. Neurochem. Int. *128*, 32–38.

Letellier, M., Wehrlé, R., Mariani, J., and Lohof, A.M. (2009). Synapse elimination in olivo-cerebellar explants occurs during a critical period and leaves an indelible trace in Purkinje cells. Proc. Natl. Acad. Sci. U.S.A. *106*, 14102–14107.

Leto, K., Arancillo, M., Becker, E.B.E., Buffo, A., Chiang, C., Ding, B., Dobyns, W.B., Dusart, I., Haldipur, P., Hatten, M.E., et al. (2016). Consensus Paper: Cerebellar Development. Cerebellum *15*, 789–828.

Lewis, T.L., Courchet, J., and Polleux, F. (2013). Cell biology in neuroscience: Cellular and molecular mechanisms underlying axon formation, growth, and branching. J. Cell Biol. *202*, 837–848.

Liu, R.Y., and Snider, W.D. (2001). Different signaling pathways mediate regenerative versus developmental sensory axon growth. J. Neurosci. *21*, RC164.

Lohof, A.M., Mariani, J., and Sherrard, R.M. (2005). Afferent-target interactions during olivocerebellar development: Transcommissural reinnervation indicates interdependence of Purkinje cell maturation and climbing fibre synapse elimination. Eur. J. Neurosci. *22*, 2681–2688.

Mayanil, C.S., George, D., Mania-Farnell, B., Bremer, C.L., McLone, D.G., and Bremer, E.G. (2000). Overexpression of murine Pax3 increases NCAM polysialylation in a human medulloblastoma cell line. J. Biol. Chem. *275*, 23259–23266.

Meeker, R., and Williams, KS (2015). The p75 neurotrophin receptor: at the crossroad of neural repair and death. Neural. Regen. Res. *10*, 721–725.

Nishiyama, H., Fukaya, M., Watanabe, M., and Linden, D.J. (2007). Axonal motility and its modulation by activity are branch-type specific in the intact adult cerebellum. Neuron *56*, 472–487.

Ribas, V.T., and Costa, M.R. (2017). Gene Manipulation Strategies to Identify Molecular Regulators of Axon Regeneration in the Central Nervous System. Front. Cell. Neurosci. *11*, 231.

Rodemer, W., Hu, J., Selzer, M.E., and Shifman, M.I. (2020). Heterogeneity in the regenerative abilities of central nervous system axons within species: why do some neurons regenerate better than others? Neural. Regen. Res. *15*, 996–1005.

Rossi, F., Wiklund, L., van der Want, J.J., and Strata, P. (1991). Reinnervation of cerebellar Purkinje cells by climbing fibres surviving a subtotal lesion of the inferior olive in the adult rat. I. Development of new collateral branches and terminal plexuses. J. Comp. Neurol. *308*, 513–535.

Rutishauser, U. (2008). Polysialic acid in the plasticity of the developing and adult vertebrate nervous system. Nat. Rev. Neurosci. *9*, 26–35.

Schiff, M., Röckle, I., Burkhardt, H., Weinhold, B., and Hildebrandt, H. (2011). Thalamocortical pathfinding defects precede degeneration of the reticular thalamic nucleus in polysialic acid-deficient mice. J. Neurosci. *31*, 1302–1312.

Schüller, U., Kho, A.T., Zhao, Q., Ma, Q., and Rowitch, D.H. (2006). Cerebellar "transcriptome" reveals cell-type and stage-specific expression during postnatal development and tumorigenesis. Mol. Cell. Neurosci. *33*, 247–259.

Sherrard, R.M., and Bower, A.J. (2001). BDNF and NT3 extend the critical period for developmental climbing fibre plasticity. NeuroReport. *12*, 2871–2874.

Sherrard, R.M., Bower, A.J., and Payne, J.N. (1986). Innervation of the adult rat cerebellar hemisphere by fibres from the ipsilateral inferior olive following unilateral neonatal pedunculotomy: an autoradiographic and retrograde fluorescent double-labelling study. Exp. Brain. Res. *62*, 411–421.

Sherrard, R.M., Dixon, K.J., Bakouche, J., Rodger, J., Lemaigre-Dubreuil, Y., and Mariani, J. (2009). Differential expression of TrkB isoforms switches climbing fiber-Purkinje cell synaptogenesis to selective synapse elimination. Dev. Neurobiol. *69*, 647–662.

Spear, P.D. (1995). Plasticity following neonatal visual cortex damage in cats. Can. J. Physiol. Pharmacol. *73*, 1389–1397.

Sugihara, I., Wu, H., and Shinoda, Y. (1999). Morphology of single olivocerebellar axons labeled with biotinylated dextran amine in the rat. J. Comp. Neurol. *414*, 131–148.

Sugihara, I., Lohof, A.M., Letellier, M., Mariani, J., and Sherrard, R.M. (2003). Post-lesion transcommissural growth of olivary climbing fibres creates functional synaptic microzones. Eur. J. Neurosci. *18*.

Tillakaratne, N.J.K., Guu, J.J., de Leon, R.D., Bigbee, A.J., London, N.J., Zhong, H., Ziegler, M.D., Joynes, R.L., Roy, R.R., and Edgerton, V.R. (2010). Functional recovery of stepping in rats after a complete neonatal spinal cord transection is not due to regrowth across the lesion site. Neuroscience *166*, 23–33.

Uryu, K., Butler, A.K., and Chesselet, M.F. (1999). Synaptogenesis and ultrastructural localization of the polysialylated neural cell adhesion molecule in the developing striatum. J. Comp. Neurol. *405*, 216–232.

Vavrek, R., Girgis, J., Tetzlaff, W., Hiebert, G.W., and Fouad, K. (2006). BDNF promotes connections of corticospinal neurons onto spared descending interneurons in spinal cord injured rats. Brain *129*, 1534–1545.

Vennemann, A., Agoston, Z., and Schulte, D. (2008). Differential and dose-dependent regulation of gene expression at the mid-hindbrain boundary by Ras-MAP kinase signaling. Brain Res. *1206*, 33–43.

Vogelaar, C.F., Hoekman, M.F.M., Brakkee, J.H., Bogerd, J., and Burbach, J.P.H. (2004). Developmental regulation of homeobox gene expression in dorsal root ganglion neurons is not recapitulated during regeneration of the crushed sciatic nerve. Neuroscience *125*, 645–650.

Willson, M.L., McElnea, C., Mariani, J., Lohof, A.M., and Sherrard, R.M. (2008). BDNF increases homotypic olivocerebellar reinnervation and associated fine motor and cognitive skill. Brain *131*, 1099–1112.

Yin, B., Ma, Z.Y., Zhou, Z.W., Gao, W.C., Du, Z.G., Zhao, Z.H., and Li, Q.Q. (2015). The TrkB+ cancer stem cells contribute to post-chemotherapy recurrence of triple-negative breast cancers in an orthotopic mouse model. Oncogene *34*, 761–770.

Zagrebelsky, M., Strata, P., Hawkes, R., and Rossi, F. (1997). Reestablishment of the olivocerebellar projection map by compensatory transcommissural reinnervation following unilateral transection of the inferior cerebellar peduncle in the newborn rat. J. Comp. Neurol. *379*, 283–299.

Zennou, V., Serguera, C., Sarkis, C., Colin, P., Perret, E., Mallet, J., and Charneau, P. (2001). The HIV-1 DNA flap stimulates HIV vector-mediated cell transduction in the brain. Nat. Biotechnol. *19*, 446–450.

Zhang, Y., Zhang, X., Yeh, J., Richardson, P., and Bo, X. (2007). Engineered expression of polysialic acid enhances Purkinje cell axonal regeneration in L1/GAP-43 double transgenic mice. Eur. J. Neurosci. *25*, 351–361.

Zufferey, R., Nagy, D., Mandel, R.J., Naldini, L., and Trono, D. (1997). Multiply attenuated lentiviral vector achieves efficient gene delivery in vivo. Nat. Biotechnol. *15*, 871–875.

Figure 1. BDNF administration rapidly increases collateral sprouting from host climbing fibres.

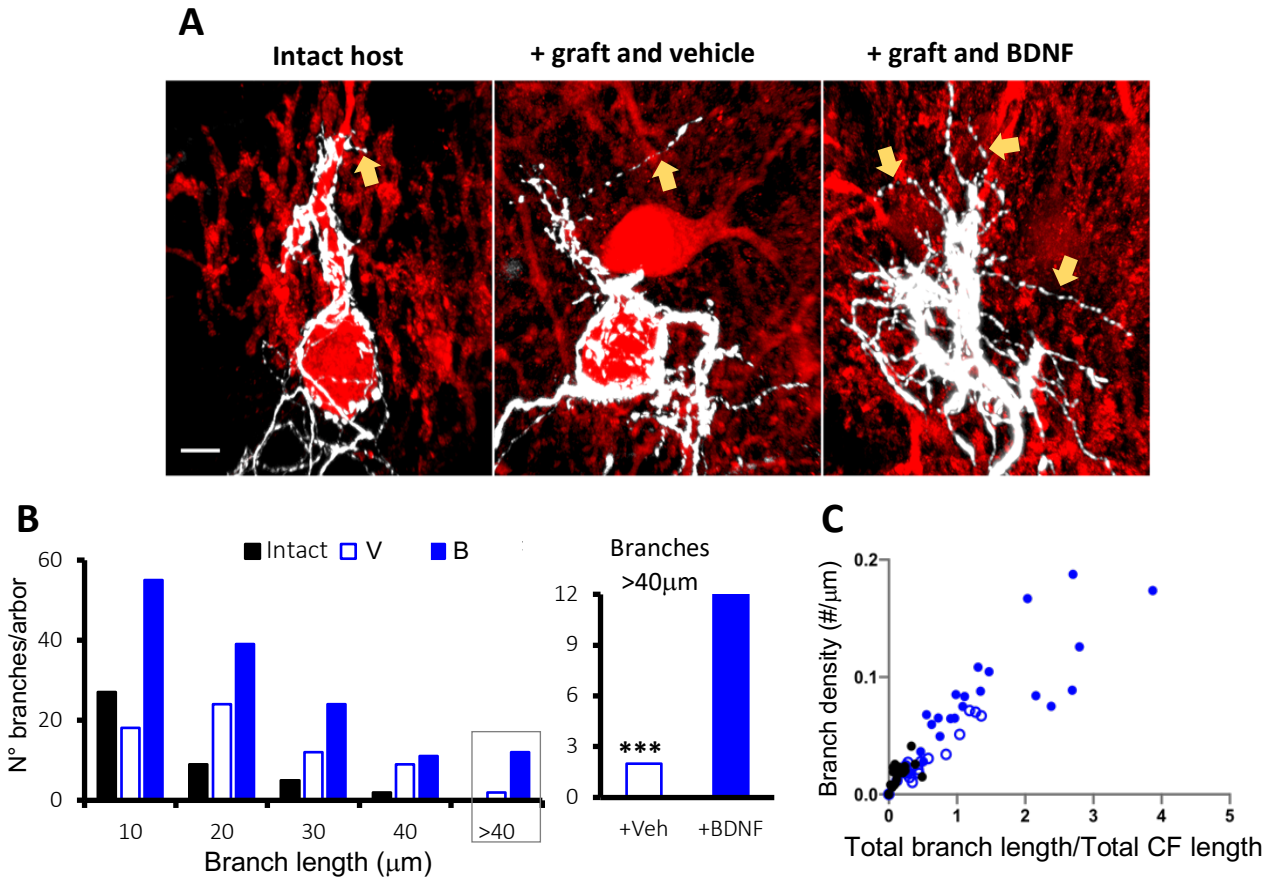

A: In the intact host cerebellar plate (left panel), horizontal branches projecting from GFP-expressing olivary climbing fibres innervate Purkinje cells. Also, thin horizontal branches of climbing fibre arbors (gold arrows) are rare. After lesion and coculture (middle panel) labelled climbing fibres of the *intact host* hemicerebellum have longer thin horizontal branches, and in the presence of BDNF (right panel) these horizontal branches of intact climbing fibres are also more numerous.

B: Quantification of horizontal climbing fibre branches in the intact host hemicerebellum 24 hours after lesion and coculture. Horizontal branches are more numerous (left panel; ANOVA $F_{2,57} = 12.7$, $p<0.0001$) and longer (ANOVA $F_{2,52} = 19.93$, $p<0.0001$) in cocultures treated with BDNF. The number of horizontal branches longer than 40 μm was significantly higher after BDNF application than vehicle-treatment or intact (non-lesioned) controls (right panel; $\chi^2 = 29.32$, df = 2, $p<0.0001$).

C: Climbing fibre horizontal branch morphology is illustrated by plotting branch density vs. total branch length/total dendrite length (de Paola et al, 2006). In comparison with normal climbing fibre horizontal branches in the intact, BDNF increases the density of longer branches

Between group post-hoc comparisons BDNF vs. vehicle: ***, $p<0.001$.

Bar = 10 μm.

Figure 2: PSA-NCAM induces olivocerebellar reinnervation

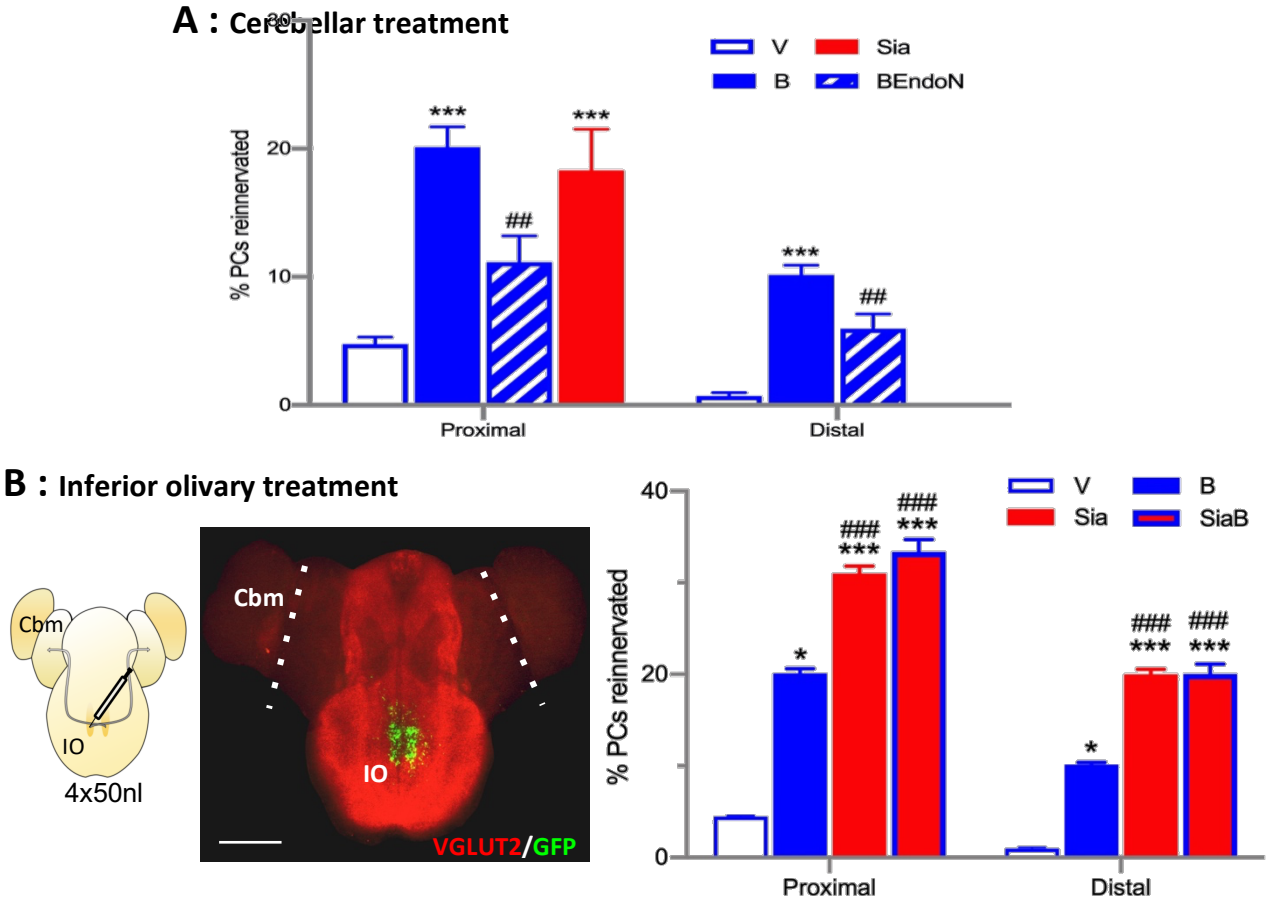

A: PC reinnervation was analysed at 10 days post-treatment. In the grafted cerebellar plate, reinnervation induced by BDNF (B) is reduced when PSA-NCAM is lysed by the sialase EndoN (B+E; ANOVA, $F_{5,59}$ = 58.49, p<0.01) in both proximal and distal zones. Also, overexpression of *sia2* in the cerebellar plate to increase PSA-NCAM, promotes CF-PC reinnervation to a similar level as BDNF (proximal zone: Sia, $F_{2,27}$ = 77,11, p<0.0001). Because lentiviral neuronal transfection is slightly variable between explants, we only analysed reinnervation in the proximal zone to avoid variability due to the injection site.

Between group post-hoc comparisons BDNF/sia vs. vehicle: ***, p<0.001.

Between group post-hoc comparisons BDNF vs. BDNF+EndoN: ##, p<0.01.

B: Lentivirus injected (4x50 nl) into the ION of explants (left panel) is detected by GFP expression (middle panel) or FLAG immunohistochemistry (not shown). The injection remains highly localised to the inferior olivary region. The white dotted line represents the junction between the host and graft hemicerebella. Bar = 1mm.

CF-PC reinnervation (right panel) in proximal and distal regions of the grafted cerebellar plate, following olivary injection of LV-Sia2 or LV-GFP with (SiaB, B) or without (Sia, V) BDNF applied to the grafted cerebellar plate. In both proximal and distal regions, *sia2* overexpression ± BDNF induced more reinnervation than BDNF or LV-GFP/Vehicle alone ($F_{3,30}$ = 119.3, p<0.0001); but the 2 treatments were not additive.

Between group post-hoc comparisons BDNF/sia/siaB vs. vehicle: *, p<0.05; ***, p<0.001.

Between group post-hoc comparisons BDNF vs. sia/siaB: ###, p<0.001.

Figure 3: Olivary *Pax3* regulates olivocerebellar reinnervation

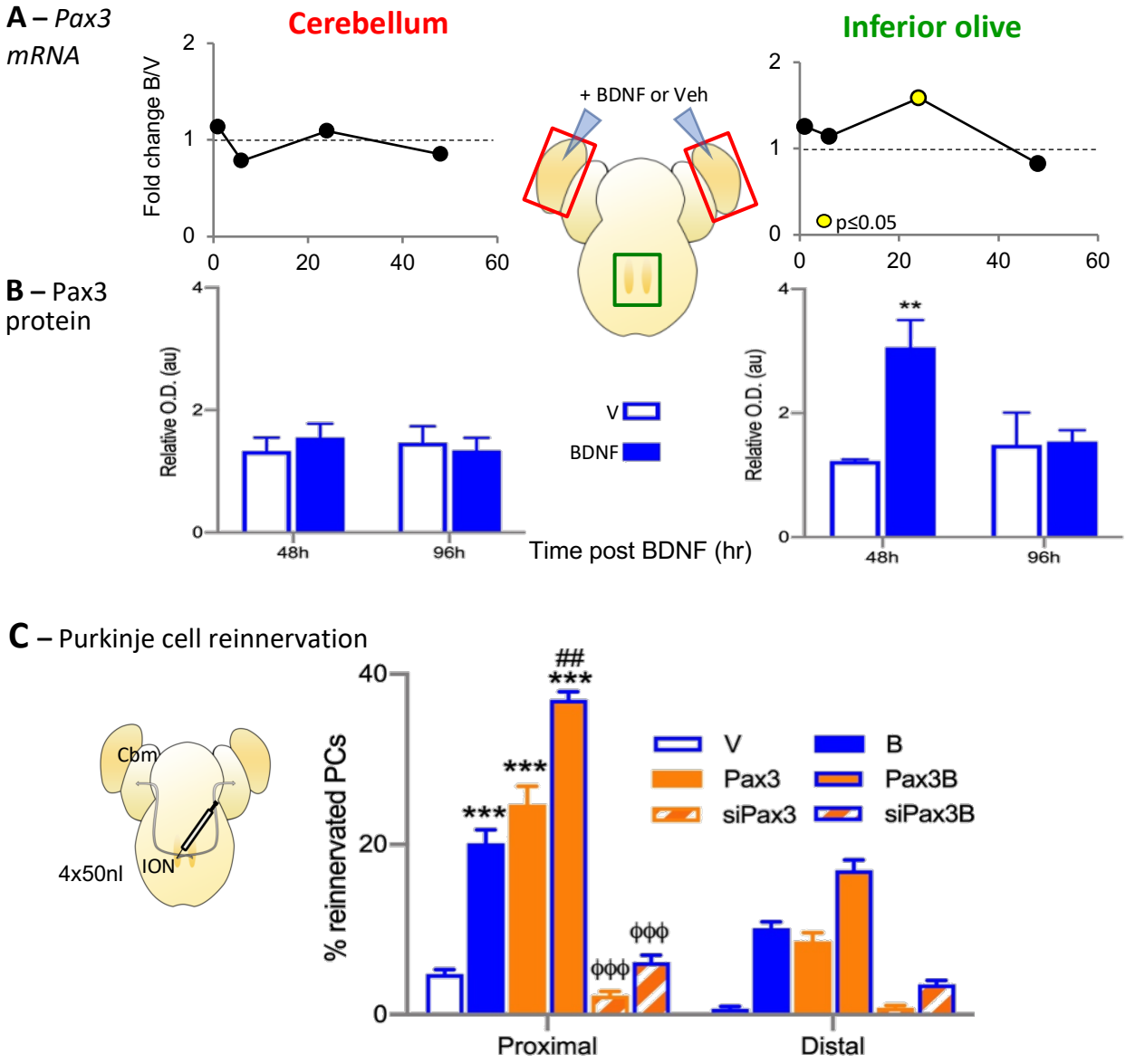

A: Quantitative PCR of the hemicerebellum or inferior olive 6-48h post lesion and coculture reveals transient *Pax3* upregulation in the inferior olive, but not the cerebellum, 24h after lesion and BDNF treatment (Kruskal-Wallis $H_{8,46}$ = 16.82, p=0.018; post-hoc MWU: 1h, p=0.55; 6h, p=0.008).

B: Western blot analysis at 48-96h post coculture also revealed a transient increase in Pax3 protein in the inferior olive after BDNF treatment (ANOVA $F_{7, 40}$ = 4,170, p=0.0016), but not in the cerebellum. However, increased Pax3 occurred at 48h post BDNF, which follows the rise in RNA (cf A).

Between group post-hoc comparisons B vs. V: **, p<0.01;

C: Modifying inferior olivary *pax3* dramatically alters climbing fibre-Purkinje cell reinnervation (2way-ANOVA, $F_{11,105}$ = 82,72, p<0.0001). Reinnervation in proximal and distal regions of the grafted cerebellar plate, following olivary injection of LV-Pax3 alone (orange bar) or with BDNF (blue border), LV-GFP with (blue bar) or without (black bar) BDNF. In both proximal and distal regions, *pax3* overexpression induced reinnervation equivalent to BDNF and more than LV-GFP/Vehicle alone ($F_{7,77}$ = 99,61, p<0.0001). The 2 treatments were additive, so that the effect of LV-Pax3 with

BDNF was greater than any single treatment (LV-Pax3 < LV-Pax3 BDNF, $p<0.01$). When *pax3* was knocked-down by LV-siPax3 (by 70%, manufacturers data), BDNF-induced reinnervation was decreased ($F_{5,47} = 58,53$, $p<0.0001$) to the percentage in vehicle treated explants.
Between group post-hoc comparisons BDNF/Pax3/Pax3+BDNF vs. vehicle: ***, $p<0.001$; Pax3 vs. Pax3+BDNF: ##, $p<0.01$; siPax3 vs. BDNF/Pax3/Pax3+BDNF: ϕϕϕ, $p<0.0001$.
NB: the statistical differences shown in the proximal zone also exist in the distal zone, but for clarity of the figure they have not been added to the graphic.

Figure 4: Pax3 increases PSA-NCAM and axonal sprouting

A – Climbing fibre terminal sprouts after inferior olivary Pax3 overexpression

B – Cerebellar PSA-NCAM

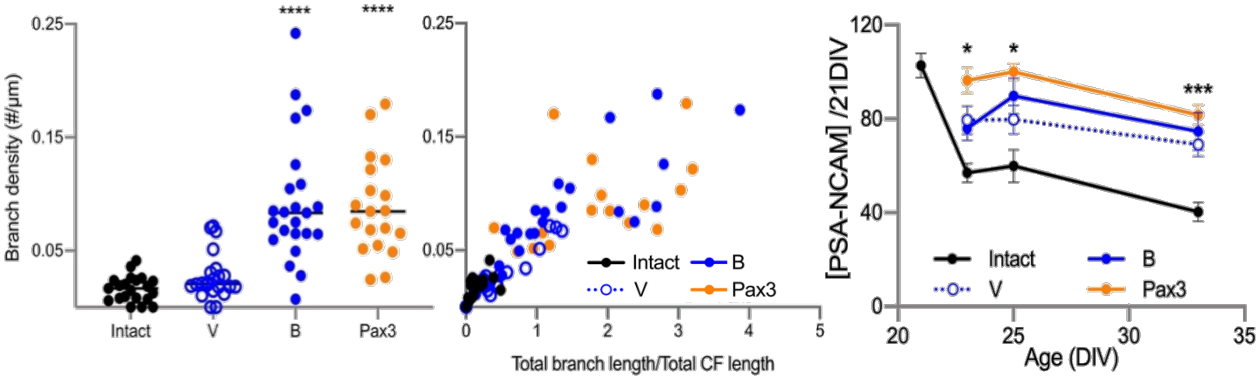

C – PSA-NCAM is on reinnervating growth cones

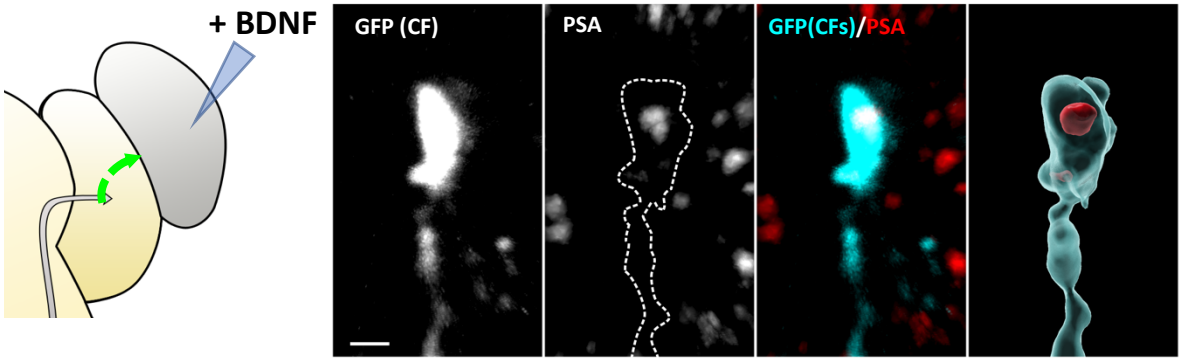

A: After lesion and co-culture at 21DIV followed 24h later by olivary LV-Pax3 injection (Pax3), climbing fibre horizontal branches increase within 24h in a manner similar to cerebellar BDNF treatment (B, left panel). There is a greater density of longer branches (Kruskal-Wallis, $H_{4,82} = 52.92$, $p<0.0001$) in BDNF (B) and Pax3 (Pax3) treated groups compared to vehicle (V; Dunn's post-hoc comparisons, intact vs. BDNF, intact vs. Pax3: both $p<0.0001$; right panel includes data from Fig 1C for comparison).

B: As a potential mechanism underlying Pax3-induced reinnervation, we observed increased cerebellar PSA-NCAM from 4 days after lesion and olivary LV-Pax3 transfection when compared to intact or lesion vehicle/LV- GFP controls ($F_{11, 117} = 6,416$, $p<0.0001$) and this was sustained at 12 days post lesion.

C: In the host cerebellar plate 2 days after lesion/co-culture and BDNF treatment (left-hand schema), a GFP-labelled olivary axon growth cone, GFP (CF), expresses PSA-NCAM. The right-hand panel is a 3D construction from the z-stack confirming the PSA-NCAM (red) on the growth cone. Bar = 1 µm.

Comparisons to intact tissue: *, $p<0.05$; ***, $p<0.001$; ****$p<0.0001$

Figure 5: Pax3 is involved in developmental climbing fibre-Purkinje cell reinnervation

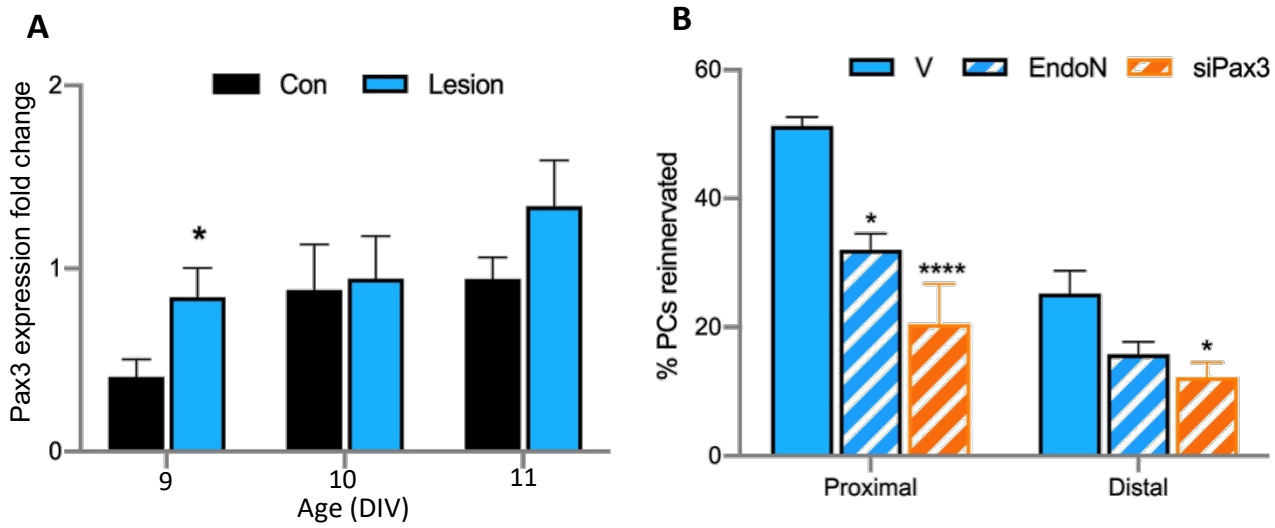

A: Post lesion and co-culture at 9DIV (~P3), *Pax3* expression increases very rapidly in the inferior olive (Two-way ANOVA, $F_{2,13} = 4.67$, p=0.03), so that at 6h post-lesion there is a 2-fold greater *Pax3* expression compared to controls. This level then remains stable during the period of reinnervation. N=5 olivary regions for each group.

B: Explants were lesioned and co-cultured at 9DIV (~P3). The cerebellar plate was then treated with vehicle (V), or EndoN to lyse PSA from NCAM (EndoN), or the inferior olive was injected with LVsiPax3 (siPax3), to knock-down Pax3 expression. The amount of Purkinje cell reinnervation was significantly reduced by both treatments (ANOVA, EndoN: $F_{3,34} = 33.33$, p<0.0001; LVsiPax3: $F_{3,28} = 14.7$, p<0.0001). Number of cerebellar plates per group: V = 10, EndoN = 9, siPax3 = 6.
Comparisons to vehicle-treated: ** = p<0.01; *** = p<0.0001

TABLE 1: PSA-NCAM concentration in the cerebellum and inferior olive during development and olivocerebellar reinnervation.

Table 1a : Cerebellar PSA-NCAM concentration (AUs; mean±SEM, n=cerebellar plates)

DIV	Age	Control	Vehicle	BDNF	BDNF+EndoN	BDNF isolated
9	3	114.7±10.2 (4)				
13	7	113.3±10.2 (5)				
21	15	102.8±5.1 (5)				
24	18	57.0±3.9 (3)	80.3±7.7 (10)	76.0±4.9 (9)		
26	20	64.3±6.9 (5)	65.5±3.1 (8)	89.9±7.6 (15)	**# 42.1±10.3 (3)**	**### 44.9±9.9 (6)**
34	28	40.4±4.1 (5)	58.1±2.3 (4)	***74.6±8.0 (6)**		

Compared to vehicle * p<0.05; compared to BDNF # p<0.05, ### p<0.001

Table 1b : Inferior olivary PSA-NCAM concentration (AUs; mean±SEM, n= inf olives)

DIV	Age	Control	Vehicle	BDNF	BDNF+EndoN
9	3	82.1±11.3 (6)			
13	7	80.8±5.2 (7)			
21	15	106.3±3.6 (5)			
24	18	40.3±3.9 (7)	78.4±7.4 (10)	77.8±5.1 (10)	
26	20	42.3±4.0 (5)	93.5±12.3 (11)	***** 96.5±11.4 (15)**	**# 59.2±22.6 (4)**
34	28	19.5±3.3 (5)	90.5±5.7 (7)	***** 119.6±14.2 (4)**	

Compared to control, *** p<0.001; compared to BDNF or vehicle, # p<0.05

PSA-NCAM decreases during maturation in the cerebellar plate (A: ANOVA $F_{5,21}$ = 20.8, p<0.0001) and inferior olivary region (B: ANOVA $F_{5,29}$ = 34.2, p<0.0001).

A: In the cerebellar plate, post lesion BDNF administration partly counters the decrease (ANOVA $F_{8,56}$ = 4.08, p=0.0007), resulting in higher PSA-NCAM tissue concentration after 12 days (post-hoc p<0.05). However, BDNF does not increase PSA-NCAM in an isolated cerebellar plate (BDNF isolated), where reinnervation cannot take place, (post hoc p<0.001), or when the sialase EndoN (BDNF+EndoN) is added to lyse PSA from NCAM (post-hoc p<0.01) resulting in less PSA-NCAM than in the lesion/coculture/BDNF cerebellum.

B: In the inferior olive BDNF treatment increased PSA-NCAM (ANOVA $F_{9,69}$ = 17.2, p<0.0001), but this was abolished by EndoN (BDNF+EndoN) compared to vehicle or BDNF alone (both, p<0.05).

Supplementary Material for Jara et al

Figure S1: Climbing Fibre reinnervation *in vitro*

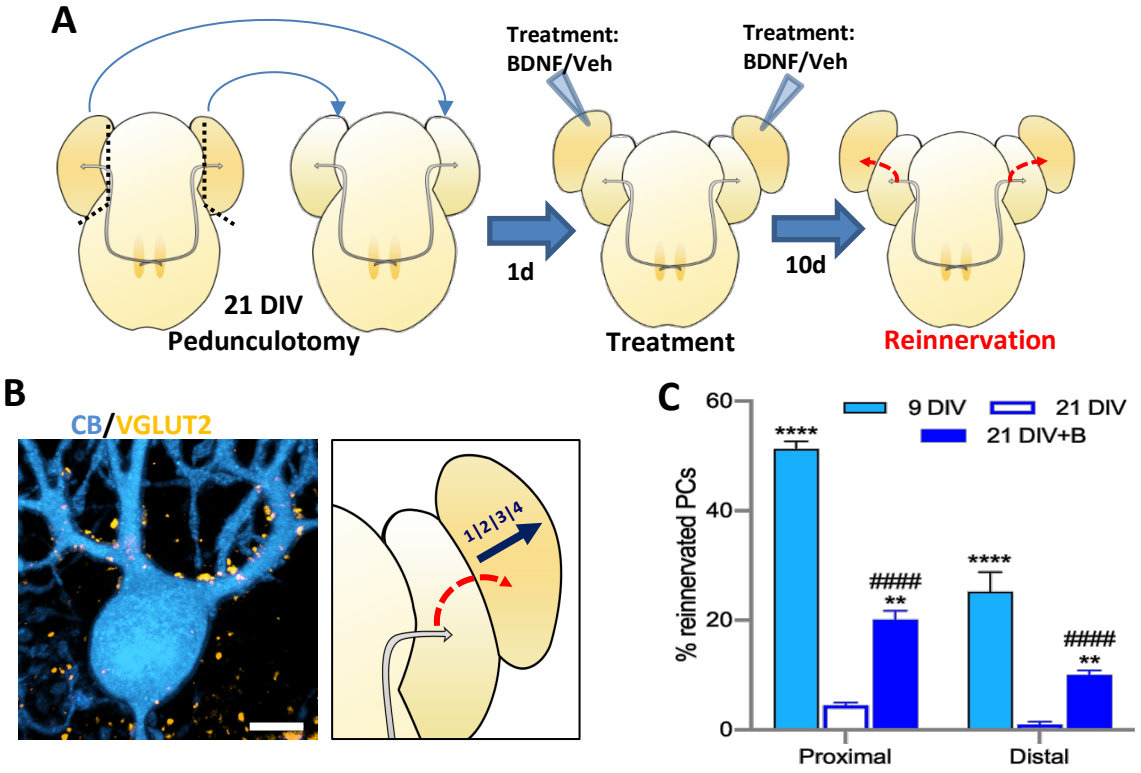

Post-lesion climbing fibre (CF) reinnervation in an *ex vivo* model of the olivocerebellar path mimics *in vivo* repair (Dixon and Sherrard, 2006; Willson et al., 2008).

A: The E14 mouse hindbrain containing the cerebellum and inferior olivary nucleus is isolated and cultured in "open-book" configuration. Isolated (denervated) cerebellar plates are positioned next to host (intact) cerebella to provide denervated target Purkinje cells (PCs) for reinnervation by the intact olivocerebellar axons (grey arrows). Grafted cerebellar plates can be treated with BDNF or vehicle to induce reinnervation (red dotted arrows).

B: Immunostaining for calbindin (CB, PCs) and VGLUT2 (CFs) allows quantification of CF reinnervation in the grafted cerebellar plate following BDNF or lentivirus application to the denervated tissue. CB/VGLUT2 co-labelled PCs are counted on image z-stacks taken in rows with increasing distance from the host (rows 1 to 4). Rows 1 and 2 form the proximal zone; rows 3 and 4 the distal zone. Bar = 10μm.

C: Reinnervation of PCs in the grafted cerebellar plate is extensive after lesion at 9 DIV (equivalent to P3) and, following lesion at 21DIV (equivalent to P15), is significantly higher if BDNF is applied (21 DIV+B) compared to vehicle-treated controls (Kruskall-Wallis KW $_{6,69}$ = 63.7, p<0.0001).
Comparison vs. 21 DIV: ****, p<0.0001; **, p<0.01 ; comparison vs. 9 DIV lesion, ####, p<0.0001.

Figure S2: BDNF action is restricted to the injected graft hemicerebellum

To examine the spread of BDNF into the host hemicerebellum, we used *c-fos* expression to detect BDNF action.

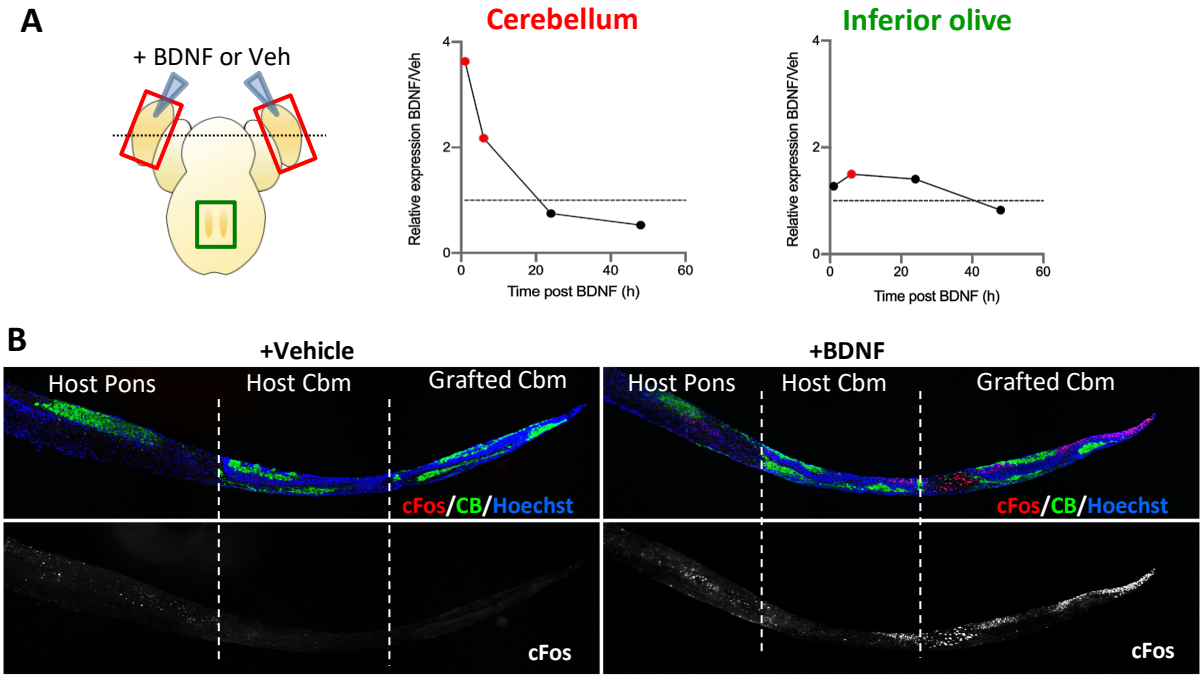

A: The diagram (left) shows which tissue was analysed: red squares indicate cerebellar tissue and the green square inferior olive tissue taken for qPCR. The black dotted line shows the orientation of frontal sections of the fixed explant in B. *Cfos* expression fold-change in the cerebellum and inferior olive after BDNF treatment. The horizontal dotted line indicated the control expression in intact host tissue. At 1h post BDNF, there is a 4-fold increase of cerebellar *cfos* (red circle, $p<0.001$), which is still raised at +6h (red circle, $p<0.01$) but has returned to baseline at +24h. In contrast, there is only a small increase in olivary *cfos* 6h after BDNF treatment (red circle, $p<0.01$).

B: Immunolabelling shows c-fos (red) after BDNF application to the graft (right panels) but none after vehicle treatment (left panels). In the BDNF-treated explant, c-fos labelling is essentially in the graft cerebellum (right) with minimal expression at the edge of the adjacent host hemicerebellum (centre) and none in the host brainstem (left). This is consistent with the strong cerebellar expression of TrkB receptors (Bosman et al., 2006; Sherrard et al., 2009) limiting BDNF spread.

The vertical dotted lines indicate the separations between the different areas of the explant.

Figure S3: Cerebellar injection of LV-Sia2 does not transfect Purkinje cells

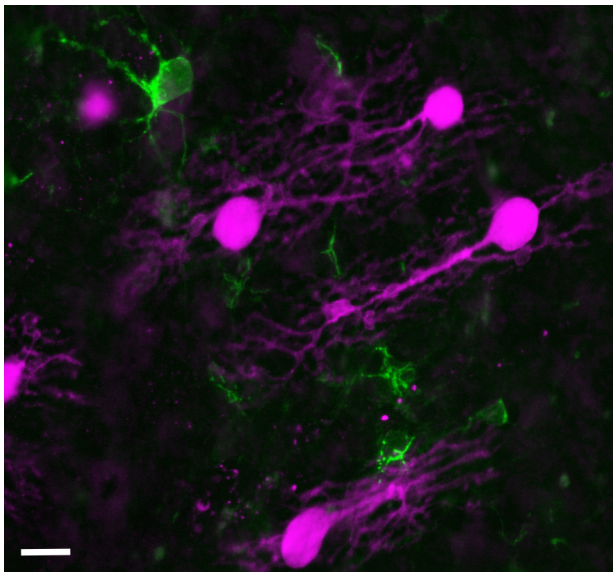

Flattened Z-stack image of the explant hemi-cerebellum after injection of LV-Sia2 counterstained with calbindin to label Purkinje cells (magenta). LV transfection is revealed by Flag expression (green) and this does not co-localize with calbindin. This suggests that any PSA-NCAM synthetized through *Sia2* expression acts through providing a growth permissive cellular environment and does not need to be specifically expressed by target Purkinje cells.
Bar = 20μm.

Figure S4: LV-Sia4, 3'UTR-Sia2 and 3'UTR-Sia4 induce olivocerebellar reinnervation

In contrast to LV-Sia2, the effect of LV-Sia4 on CF-PC reinnervation was less pronounced, inducing similar reinnervation to BDNF ($F_{8,65}$ = 69.9, p<0.0001) and less than LV-Sia2 (p<0.001). However, the percentage of PC reinnervation increased when LV-Sia4 and BDNF were combined (Sia4B > Sia4; p<0.01) to equal that induced by LV-Sia2 +/- BDNF (Sia, SiaB). Since Sia4 is expressed preferentially in the mature nervous system, specifically in regions of synaptic plasticity (Rutishauser, 2008; Uryu et al., 1999), its induction of less reinnervation than Sia2 is consistent with different roles for these two enzymes in the developing/mature nervous system.

Given the large distance between the medullary inferior olive and sprouting cerebellar CF axon terminals, we tested whether targeting the upregulated mRNA to the axon terminal would produce a greater effect. However, inferior olivary injections of LV-Sia2-3'UTR (Sia3') or LV-Sia4-3'UTR (Sia43') in lesioned co-culture explants had only the same effect as the non-3'UTR vectors.

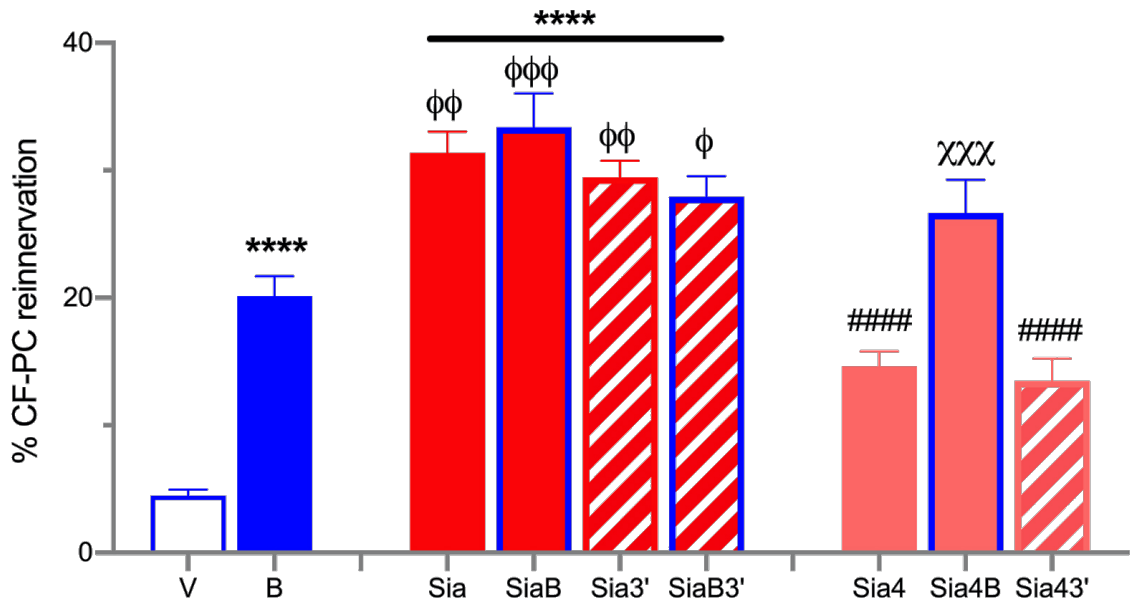

Bars show mean ± SEM

Compared to vehicle **** p<0.0001;
Compared to Sia2, ####, p<0.0001
Compared to BDNF, ϕ p<0.05; ϕϕ p<0.01; ϕϕϕ p<0.001
Compared to Sia4 and Sia43', χχχ p<0.001

Figure S5: Biological pathways linking BDNF and Pax3

A potential link between BDNF and PSA-NCAM, which is synthesised through the action of sialtransferases *Sia2* and *Sia4*, is the transcription factor Pax3 (Mayanil et al., 2000). It is known that in cerebellar neuronal culture BDNF upregulates *Pax3* (Kioussi and Gruss, 1994), which is expressed in the immature cerebellum and brainstem (Schüller et al., 2006; Vennemann et al., 2008). Also, BDNF-TrkB signalling induces Klf4 (Yin et al., 2015) and Stat3 (Kamaraju et al., 2002), both of which bind to response elements in the *Pax3* promoter. Moreover, BDNF has direct protein-protein interactions leading to the Pbx1/Meis2 complex (Grados et al., 2014) that directly induces *Pax3* expression (Chang et al., 2008). We used *in silico* searches to confirmed these links.

A: Diagram showing BDNF and Pax3 protein-protein interactions from the STRING database with an interaction score of >0.8

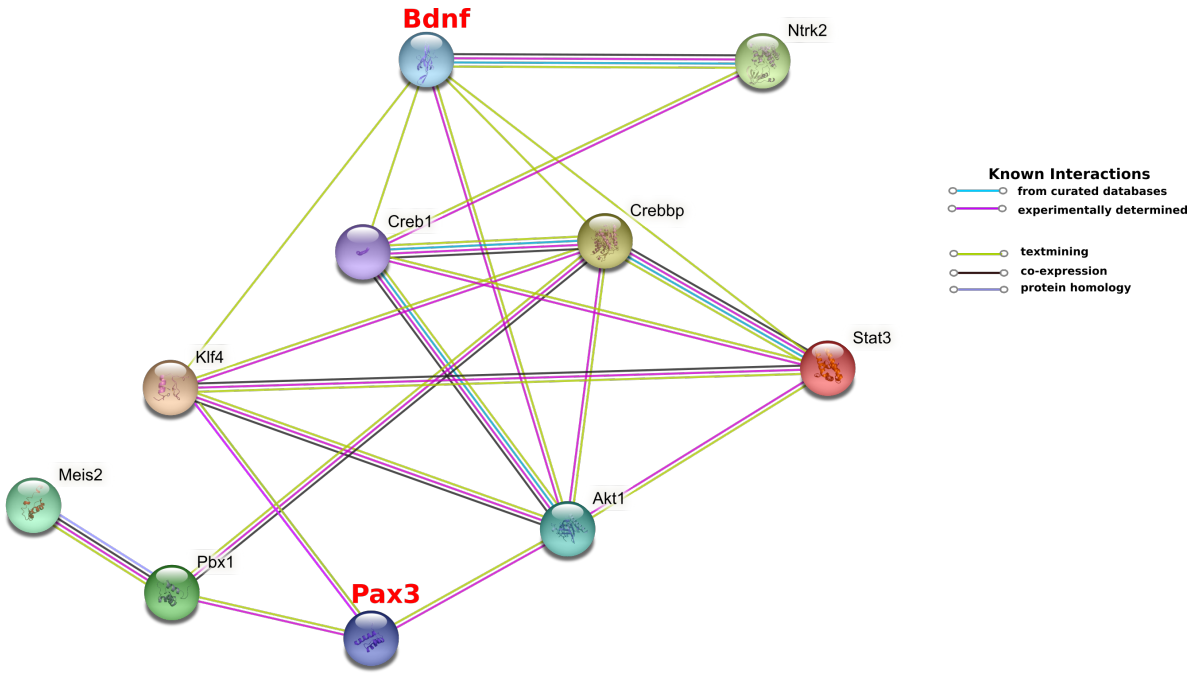

B: To clarify that Pax3 was capable of inducing axonal outgrowth and olivocerebellar reinnervation, we searched Gene Ontology functions of interest (axon extension, GO:0048675; axon regeneration, GO:0031103; and synapse, GO:0051963) for genes containing predicted Pax3 binding elements. (see Excel file Jara_Pax3 target genes). The position weight matrix for Pax3 (top left) indicates the probability of specific bases at each position within the response elements. We then used PubMed text mining to identify potential Pax3-targets which are expressed in the olivocerebellar system (in red bold).

Axon Regeneration

Lamb2 **Mif** Rgma Rtn4rl1
Fkbp1b **Jun** Map2k2 Stk24
Epha4 Xylt1 Klk8 **Jak2**
Mmp2 Omg Braf Apoe
Bcl2 Nefl

Axon Extension

Lamb2 **Dscam** Barhl2
Trpv2 Islr2 Twf2 Mgll Golga4
Cdkl3 **Slit2 Cxcl12 Slit1** Sema5a **Vegfa**
Wdr36 **Srf** Megf8 Ryk Lhx2 Wnt5a
Wnt3a **Wnt3** Vcl Arhgap4 **Dcx** Nkx6-1
Sema4f **Sema3f** Rab21 Nrp2
Tnfrsf12a **Usp9x** Pou4f3 Ccr5 **Aatk**
Fxn Disc1 Ep300 Cdh4 **Apoe**
Ntn1

Synapse formation

Ntrk2 Agrn **Mecp2** Chrnb2 **Epha5**
Ephb2 T pbg **Nlgn1** Rab17 Bhlhb9
Lingo2 Ghsr Thbs2 Nlgn2 Clstn2
Ube2v2 Xlr4b Musk Slitrk3 **Wnt7a**
Wnt5a Slitrk1 Amigo2 Ptk2 **Cbln1**
Pdlim5 Lrtm1 **Mef2c** Lrrtm3
Lrrtm2 Lrrtm1 Oxtr Cux2 Flrt1
Colq **Grin1** Nrxn3

Figure S6: Pax3-induced olivocerebellar reinnervation forms functional climbing fibre-Purkinje cell synapses.

Because inducing axonal growth and reinnervation is a new function for Pax3, it was important to confirm that the VGLUT2-labelled terminals contacting cerebellar PCs were in fact functional climbing fibre synapses.

A: Whole-cell PC recordings (see Supplementary Methods, below), in the graft cerebellar plates of explants overexpressing olivary *Pax3,* allowed us to find PCs with characteristic CF synaptic currents (CF-EPSCs), showing classic all-or-none activity and paired-pulse depression. Other PCs had no CF-EPSCs.

B: Histological analysis revealed that CF-EPSC-positive PCs, identified with biocytin-Alex Fluor488, colocalised with VGLUT2-positive profiles (red; white arrows indicate co-localisation). PCs without recorded CF-EPSCs generally did not have associated VGLUT2 labelling.

Bar = 20 μm

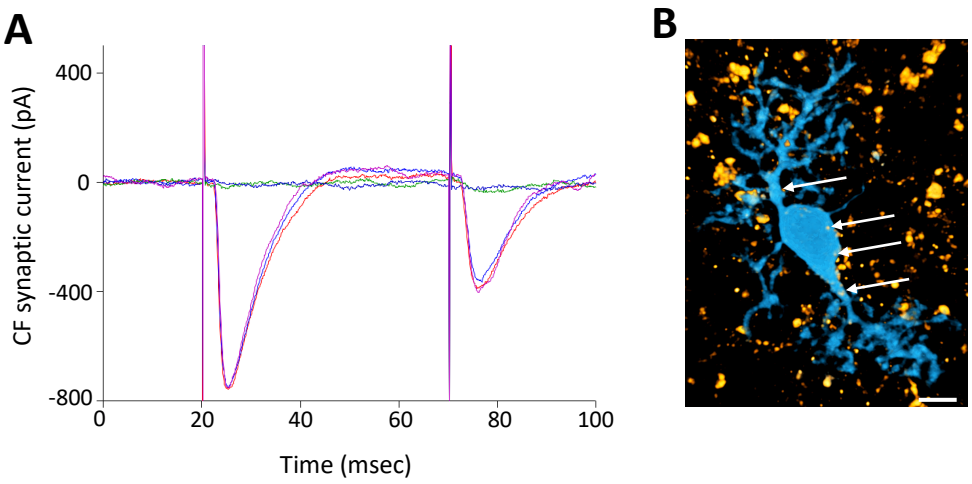

Supplementary Methods

Recombinant lentiviral vector production

Recombinant plasmid vectors encoding for *sia2, sia2-3'UTR, sia4, sia4-3'UTR, pax3 or enhanced green fluorescent protein (GFP)* under the control of the PGK promoter were used to prepare stocks of lentiviral particles as previously described (Zennou et al., 2001). All constructs were FLAG-tagged to allow for the identification of transduced cells using a FLAG antibody. Briefly, HEK 293T cells were transiently cotransfected with the p8.91 encapsidation plasmid (Zufferey et al., 1997), the pHCMV-G (Vesicular Stomatitis Virus pseudotype) envelope plasmid and the pFlap recombinant vectors containing the transgene. The supernatants were collected 48 hours after transfection, treated with DNAseI (Roche Diagnostics) and filtered before ultracentrifugation. The viral pellet was then resuspended in PBS, aliquoted and stored at -80°C until use. The amount of p24 capsid protein was determined by the HIV-1 p24 ELISA antigen assay (Beckman Coulter, Fullerton, CA). Virus from different productions averaged 175 ng/µl of p24 antigen.

Electrophysiology

Whole-cell patch-clamp recordings from Purkinje cells in explants were performed as previously described (Letellier et al., 2009)). Patch pipettes were filled with a solution containing: 120 mM Cs-D-Gluconate, 13 mM biocytin, 10 mM HEPES, 10 mM BAPTA, 3 mM TEACl, 2 mM Na2ATP, 2 mM MgATP, 0.2 mM NaGTP, pH 7.3, 290–300 mM mOsm. Explants were continuously perfused with a bath solution containing: 125 mM NaCl, 2.5 mM KCl, 1.25 mM NaH2PO4, 26 mM NaHCO3, 2 mM CaCl2, 1 mM MgCl2, 25 mM glucose, and bubbled with 95% O2 and 5% CO2. Picrotoxin (100 µM) was added to block inhibitory currents. Climbing fibre-EPSCs were elicited by stimulation with a saline-filled glass pipette in the area surrounding the Purkinje cell. We distinguished climbing fibre-EPSCs from currents mediated by parallel fibres (PF-EPSCs) by their all-or-none character and by the demonstration of paired-pulse depression.

Following electrophysiological recordings, explants were fixed in 4% paraformaldehyde (PFA) in PB 0.1 M and processed for immunohistochemistry; the recorded (biocytin-filled) Purkinje cells were visualized after incubation with AF488-conjugated avidin (Invitrogen, Molecular Probes).

Table S1: Primary antibodies used

Protein	Concentration	Species	Source
Calbindin D28K (CB)	1:5000	mouse or rabbit	Swant, Switzerland
Parvalbumin	1:5000	goat	Swant
vesicular glutamate transporter-2 (VGLUT2)	1:2000	guinea-pig or mouse	Chemicon
GFP	1:100	rabbit	Millipore
Forkhead box protein P2 (FOXP2)	1:300	rabbit	Abcam
Forkhead box protein P2 (FOXP2)	1:2000	goat	Abcam
Flag	1:2000	mouse	Sigma
Pax3	1:250	mouse	R&D systems

Table S2: Primer sequences for RT-qPCR

Gene	Forward	Reverse
TUB5	GCTAAGTTCTGGGAGGTGATAAGCG	CCAGACTGACCGAAAACGAAGTTG
ARBP	TGCCAGCTCAGAACACTGGTCTA	GGGAGATGTTCAGCATGTTCAGCA
CFOS	GGCTTTCCCCAAACTTCGACCAT	AGACGGACAGATCTGCGCAAAA
PAX3	AGCAAACCCAAGCAGGTGACA	AGGATGCGGCTGATAGAACTCACT